Modeling of the plasma jet of a stationary plasma thruster

L. Garrigues,[a] J. Bareilles, and J. P. Boeuf
CPAT, Université Paul Sabatier, 31062 Toulouse Cedex, France

I. D. Boyd
Department of Aerospace Engineering, University of Michigan, Ann Arbor, Michigan 48109-2140

(Received 13 December 2001; accepted for publication 1 April 2002)

We have developed a two-dimensional hybrid fluid – particle-in-cell Monte Carlo collisions (PIC-MCC) model to study the plume of a stationary plasma thruster. The model is based on a fluid description of the electrons (the electron density follows a Boltzmann distribution) and a particle description of the ion and neutral transport. Collisions between heavy species are taken into account with a Monte Carlo method. The electric field is obtained from Poisson's equation or from the quasineutrality assumption. We first show that the results from the PIC-MCC model are close to the results of a more time-consuming direct simulation Monte Carlo approach. We then compare the model predictions of the plume density and ion energy distribution with experimental measurements. Finally, we present a brief discussion on the assumptions of the model and on its ability to give reliable predictions on important issues such as the flux of ions backscattered to the satellite. © *2002 American Institute of Physics.* [DOI: 10.1063/1.1480480]

I. INTRODUCTION

In stationary plasma thrusters (SPT), or Hall thrusters, a plasma is created in a channel between two concentric dielectric cylinders. Xenon is injected at the anode, at one end of the channel, and is ionized by electrons injected at the other hand of the channel (exhaust). The cathode is located outside the channel, next to the exhaust plane. A system of coils and a magnetic circuit generate a large radial magnetic field in the exhaust region. The electron conductivity is low in the exhaust region because of the large magnetic field perpendicular to the cathode-anode path. Consequently, the axial electric field increases to maintain current continuity and accelerates the ions outside the channel. The Xe^+ ions are collisionless in the thruster and their mean energy at the exhaust is close to the applied voltage (on the order of 250 eV). The ion jet is neutralized by electrons coming from the cathode. Hall thrusters are well suited for geostationary satellite station keeping[1] and seem very attractive and competitive when combined with chemical thrusters[2,3] for orbit transfer mission. Engines are being studied for operation at various power and thrust levels (larger specific impulse for station-keeping mission and larger thrust for orbit transfer).[4]

In parallel to the experimental[5] and modeling[6] research effort toward a better understanding and optimization of the thruster, work is also necessary to characterize the SPT plume. The plume consists of heavy particles ejected from the thruster which can interact with the spacecraft. Effects like mechanical interaction of the plume with solar arrays, sputtering of solar arrays due to energetic ions, and contamination due to erosion products (from solar cells or thruster walls) can strongly affect the operation of the satellite and reduce its lifetime.

In this article, we do not deal with the modeling of the thruster channel itself. The aim of this article is the development of a fast and reliable two-dimensional (2D) model of the plasma jet in order to study the plasma plume and its interaction with the satellite due to backscattered ions. The ion distribution at exhaust is an input parameter of the plume model. The influence of this distribution on the plume properties (plasma density, beam divergence) is discussed in this article. A complete model including the thruster channel and the plasma jet is under development and will be presented in a future paper. The present article is associated with the launch of an experimental satellite STENTOR by CNES in 2002 with a diagnostic package on board.[7] In-orbit experiments will characterize the SPT plume and its interactions with the spacecraft. The results of our model will be compared to these measurements.

The plasma jet model is described in Sec. II. Comparisons between this model and a more complicated direct simulation Monte Carlo (DSMC) method are presented in Sec. III. Comparisons with experimental results in the French testing facility PIVOINE are described in Sec. IV. The consequences of the model assumptions are discussed in Sec. V.

II. PLUME MODEL

In this model the electrons are described as a fluid, assuming a Boltzmann law for the electron density with a constant electron temperature (typically 2–4 eV) while the ions are described with a particle-in-cell Monte Carlo-collisions (PIC-MCC) method. The electric field can be deduced from a self-consistent solution of Poisson's equation or assuming quasineutrality. In the model of Van Gilder, Boyd, and Keidar[8] a direct Monte Carlo simulation (DSMC) method is used to treat collisions, i.e., the ions and neutral atoms are followed simultaneously. In a DSMC method the influence of ion-neutral collisions on the velocity distribution of neutral atoms it taken into account self consistently. In our simulation, the collisions are treated with a classical Monte Carlo

[a]Electronic mail: garrigues@cpat.ups-tlse.fr

(MCC) method. The neutral atoms expansion is first simulated with a MCC simulation, assuming a given velocity distribution of the atoms in the exhaust plane. Due to the divergence of the flow, the neutral atom density decreases quickly away from the thruster. Far from the thruster, the neutral atom density averaged over a sphere of radius R must be proportional to $1/R^2$ and to a constant coefficient depending on the angular distribution at exhaust. Under the conditions used in this article, this average neutral density drops by two to three orders of magnitude in the simulation domain (dimension on the order of 1 m) when the background pressure is zero.

Knowing the neutral atom density, we run the PIC-MCC simulation of the plume without changing the neutral atom density. We therefore neglect the effects of the Xe^+–Xe and Xe^{++}–Xe collisions on the neutral density distribution in the plume. The collision frequency is supposed to depend only on the ion velocity (typically 100 times larger than the neutral velocity). Elastic and charge-exchange collisions between neutral atoms and singly or doubly charged ions are considered. We can also optionally take into account elastic collisions between the xenon atoms emitted by the thruster and the xenon atoms corresponding to the residual pressure in the chamber of on-ground facilities. The residual gas density gas is assumed constant at a given temperature (300 K). The different collisions cross sections are summarized in Ref. 9. Other collision processes like Coulomb collisions are negligible.[10]

The energy and angular distribution of the ions and neutral atoms at the exhaust are supposed to be known and are used as input of the simulation. We use typically 100 000 and macroparticles to simulate the singly and the doubly charged ions, and 50 000 macroparticles for the atoms. The computational domain is cylindrical, and is 1 m in the axial direction and 50 cm in the radial direction (see Fig. 1). A fixed number of macroparticles is introduced at the exhaust at each time step of the simulation. Particles reaching the boundaries of the domain are eliminated. The computational time is less than 1 h on a 1 GHz PC to obtain a stationary solution (no attempt has been made to optimize the computation time).

After each integration time step for ion transport, Poisson's equation

$$\Delta V = -\frac{e}{\varepsilon_0}(n_i - n_e) \tag{1}$$

is solved, assuming that the electron density follows a Boltzmann distribution with constant temperature T_e

$$n_e(x,r) = n_0 \exp\left[\frac{e[V(x,r)-V_0]}{k_B T_e}\right]. \tag{2}$$

The ion density at each time step, n_i, is deduced from the Monte Carlo simulation of ion transport. n_0 and V_0 are reference electron density and plasma potential, and are defined in the exhaust plane. The boundary conditions for Poisson's equation are such that the electric field perpendicular to the boundaries of the simulation domain is zero. The potential is supposed to be zero on the thruster surface, and is equal to V_0 in the exhaust plane (V_0 is set to zero in the calculations below). The electron density in the exhaust plane n_0 is equal to the ion density n_i. In order to ensure convergence at large time steps (on the order of the Courant–Friedricks–Lewey (CFL) time step for ion transport), the electron density in Poisson's equation is linearized.

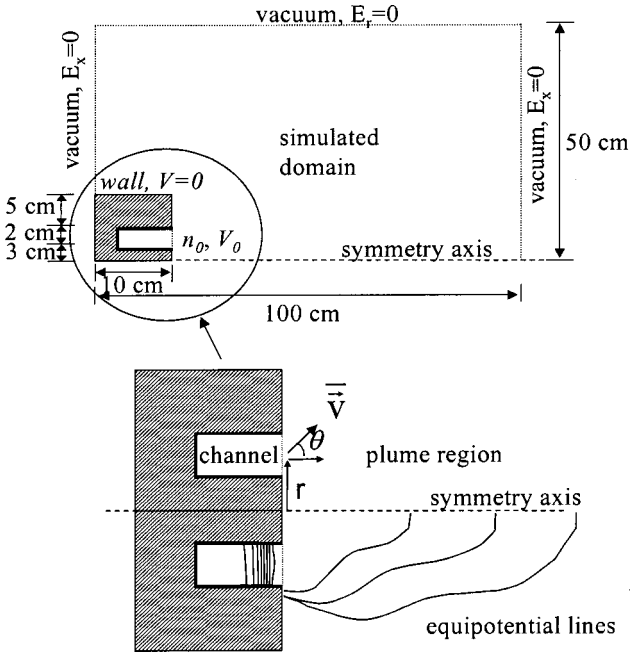

FIG. 1. simulation domain and definition of velocity vector and angle of injection in the thruster exhaust plane. Only the region outside the thruster channel (plume or plasma jet) is simulated in the present article. The energy and angular distribution of ions ejected from the channel are input parameters of the plume model.

A simpler approach, based on the quasineutrality assumption is also possible. In that case, Poisson's equation is no longer solved, and the potential distribution is simply deduced from the Boltzmann distribution above, assuming that the electron density is equal to the ion density deduced from ion transport. This simpler approach is valid provided that the electron Debye length at any point of the simulation domain is very small compared with the dimensions of the domain. We will briefly discuss below the validity of this assumption for our conditions.

In this article, we assume (as in Ref. 11) that the ion flux velocity distribution function in the exhaust plane is of the form

$$\phi(r,\vec{v}) = A v_x \exp\left[-\frac{M}{2k_B T_i}(v_x - \overline{v_x})^2\right] \times \exp\left[-\frac{M}{2k_B T_i}(v_y - \overline{v_y})^2\right] \exp\left[-\frac{M}{2k_B T_i} v_z^2\right], \tag{3}$$

where $\overline{v_x} = v_0 \cos[\theta(r)]$ and $\overline{v_y} = v_0 \sin[\theta(r)]$. M is the ion mass, and k_B is Boltzmann's constant.

The constant A is adjusted so that the total ion current in the exhaust plane is equal to a given value. The ion density n_i in the exhaust plane is assumed radially constant (and is related to A and equal to n_0) as in the model of VanGilder, Boyd, and Keidar,[8] Oh *et al.*,[12] Qarnain and Martinez-Sanchez[13] assume a radial variation of the ion den-

sity according to measurements of ion current density on a SPT-70.[14] The reliability of the experimental data is however questionable since they are deduced from intrusive probe measurements performed a few millimeters after the exhaust plane. The thruster operations and the plume properties are likely to be affected by the measurements. Due to the lack of data, some of the published results assume that the ion current distribution measured in a given thruster (e.g., SPT-70) can be extrapolated to another device (SPT-100). This is also questionable because of the sensitivity of the thruster properties to the specific geometry and magnetic-field configuration. Since we do not have reliable data concerning the ion energy distribution in the exhaust plane in our thruster, we will test several assumptions on these distributions [based on Eq. (3)]. We will also discuss the sensitivity of these assumptions on the results.

The velocity v_0 is a given constant and $\theta(r)$, in our model, is a given function of the radial position r in the exhaust plane. The assumed ion distribution in the exhaust plane is a displaced Maxwellian with temperature T_i and mean ion velocity $\vec{v}$ (modulus v_0, angle θ with respect to the thruster axis, θ depending on the radial position—see Fig. 1 for notations). Only the angle between the mean ion velocity and the thruster axis is supposed to depend on the radial position in the exhaust plane. This is a simple way to describe the possible divergence of the ion beam emitted by the thruster. T_i describes the dispersion of the ion-beam energy. Since the directed energy of the ion beam is much larger than its thermal velocity, T_i was taken to be a few electron volts while $\frac{1}{2}Mv_0^2$ was on the order of the thruster voltage. Several forms of the function $\theta(r)$ have been tested (see results below). The same analytical form [Eq. (3)] is used for neutral atoms, with T_i and v_0 replaced by the atom temperature T_a and the atom-directed velocity in the thruster, v_{0a}. The neutral atom density in the exhaust plane is assumed to be radially uniform and is deduced from the known xenon mass flow rate and ion current at exhaust by imposing the continuity relation

$$I_{a,\text{anode}} = I_{a,\text{exhaust}} + I_{i,\text{exhaust}}, \tag{4}$$

where $I_{a,\text{anode}}$ and $I_{a,\text{exhaust}}$ are the equivalent atom currents (flow rate multiplied by elementary charge) at anode and exhaust, and $I_{i,\text{exhaust}}$ is the ion current at exhaust (this relation must be modified in a straightforward manner when doubly charged ions are present). This relation assumes that one ion is ejected from the thruster for each ionized atom, and therefore neglects the ion current to the walls with respect to the total ion current. Note finally that the assumption of a radially uniform atom density in the exhaust plane is probably not realistic because ionization is not radially uniform in the channel, near the exhaust region.

III. RESULTS AND COMPARISONS WITH A DSMC METHOD

In this section, we compare the PIC-MCC method used in our model with the DSMC method of Ref. 8. We also give a typical cartography of the ion density in the plasma jet.

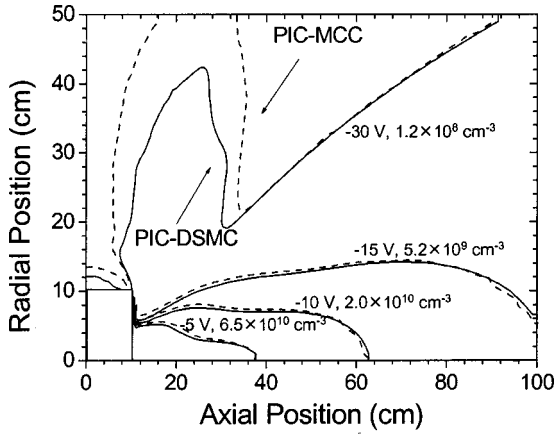

FIG. 2. Electric potential and Xe^+ density-comparisons between PIC-MCC and DSMC models. Conditions: zero background pressure, applied voltage 300 V, ion courant 3.3 A, and xenon mass flow rate 5 mg/s. The flux distribution of the ions ejected from the channel is a displaced Maxwellian with temperature $T_i = 4$ eV and mean velocity $v_0 = 1.7 \times 10^4$ m/s. The angle between the mean velocity and the thruster axis is a linear function of the radial position of the ejected ion. The flux distribution of the neutral atoms ejected from the thruster is also a displaced Maxwellian with temperature $T_a = 500$ K, and velocity $v_{0a} = 280$ m/s (same angular distribution). Electron temperature is constant and equal to 4 eV.

The thruster is schematically represented by the rectangle defined by the axial and radial positions $x = 10$ cm and $r = 10$ cm. The exhaust, i.e., the end of the thruster channel, is located on a ring of radii 3 and 5 cm at $x = 10$ cm. V_0 is set to 0 V. Typical operating conditions are: discharge current of 4.5 A; applied voltage of 300 V; and xenon mass flow rate at the anode, 5 mg/s. The ion current was assumed to be 3.3 A, i.e., 73% of the total current in the exhaust plane. With this assumption, and for an atom temperature T_a of 500 K at exhaust ($v_{0a} \sim 280$ m/s), the neutral atom density in the exhaust plane is $2.0\ 10^{12}$ cm^{-3}. The residual pressure is supposed to be zero. In these conditions the calculated atom density decreases from $2.0\ 10^{12}$ cm^{-3} in the exhaust plane to $1.0\ 10^{10}$ cm^{-3} at the end of the simulation domain, on the thruster axis (i.e., 90 cm from the exhaust plane). The ion temperature T_i and the modulus of the mean ion velocity v_0 are, respectively, 4 eV and $1.7\ 10^4$ m/s.

For this comparison, we assume a linear variation of the angle θ as a function of the radial position r (same distributions for ejected ions and neutral atoms)

$$\theta(r) = 2\theta_m(r - \overline{r})/(r_{\text{out}} - r_{\text{in}}), \tag{5}$$

where $\overline{r} = \frac{1}{2}(r_{\text{out}} + r_{\text{in}})$ is defined as the radial position at the middle of the channel, r_{out} and r_{in} are, respectively, the radial positions of the outer and inner cylinders. The value of θ_m is 10° as in Ref. 8.

We also assume that the ion beam is composed only of singly charged ions and only charge-exchange collisions between ions and atoms ejected from the thruster are taken into account in the case shown here. The electron temperature is 4 eV (probably an upper limit of the electron energy in the plume, but the aim of this section is only to compare the two methods).

We see in Fig. 2 that the agreement between PIC-MCC and DSMC models is rather good. The plasma density at the

exhaust is 3.0 10^{11} cm^{-3}. At small angles with respect to the axis, the ion density decreases as expected for a jet expansion. At larger angles, we see that the ion density profile has a local maximum. This structure in the ion density distribution is due to charge-exchange collisions between xenon ions and neutral atoms ejected from the thruster. The ions resulting from charge-exchange collisions have low energy and therefore follow the field lines towards lower potential regions. Since the potential is maximum near the exhaust, where the ion density is maximum, it is clear that some of the scattered ions going down the potential will move back toward the satellite.

Note finally that when quasineutrality is assumed, variations of plasma properties (not shown) are very similar to those obtained when Poisson's equation is solved. The main drawback with this method is the statistical noise. In regions where the number of macroparticles is low (in the zone above the SPT body), fluctuations in the number of macroparticles can induce statistical fluctuations in the calculation of the electric potential using quasineutrality.[15]

We conclude from this comparison that the accuracy of the PIC-MCC method is relatively good in the conditions of the SPT plume. As will be seen below, the accuracy of the model is limited by the uncertainties in the ion and neutral atom distributions in the exhaust plane, which lead to much larger errors than the errors introduced by the PIC-MCC method with respect to the more accurate DSMC method.

IV. COMPARISONS WITH MEASUREMENTS IN THE PIVOINE FACILITY

We have compared results obtained with the PIC-MCC model to measurements[16] performed with a retarding potential analyzer (RPA) and electrical probes in the SPT100 ML in nominal conditions. The tank background pressure of the PIVOINE facility is 2.5 m Pa (2.10^{-5} Torr) and supposed to be uniform. The electron temperature is set to 2 eV in the calculations. This value is based on probe measurements of the electron temperature in the far field.[16] The values of temperature and velocity for atom and singly ions are the same as for the previous part. We now take into account doubly charged ions, assuming that the current of Xe^{++} represents 12% of the total ion current.[17] The modulus of the mean velocity of the doubly injected ions is supposed to be $\sqrt{2}v_0$, their temperature is the same than that of Xe^{+} (4 eV). We now assume that the angular distribution of ejected particles follows the analytical formula:

$$r \geqslant \bar{r}\ \theta(r) = \theta_m \frac{1-\exp\left[\left(\frac{r-\bar{r}}{\delta}\right)^2\right]}{1-\exp\left[\left(\frac{r_{\text{out}}-r_{\text{in}}}{2\delta}\right)^2\right]}, \qquad (6)$$

$$r < \bar{r}\ \ \theta(r) = -\theta(2\bar{r}-r).$$

The notations are the same as in Eq. (5). θ_m and δ are adjusted to obtain a qualitative agreement between calculations and the ion current-density measurements.[18] In this section, θ_m and δ are, respectively, 45° and 0.25. The xenon mass flow rate is 5 mg/s and the ion current 3.6 A. The

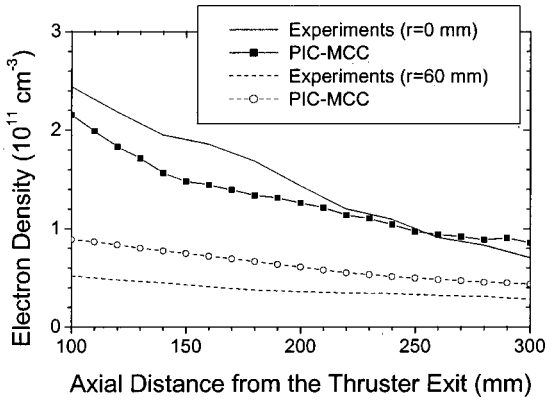

FIG. 3. Axial variations of the plasma density in the plume along the symmetry axis and 60 mm from the thruster axis: comparisons between simulation and experiments in the PIVOINE facility. Electron temperature is constant and equal to 2 eV.

neutral density of nonionized atoms is typically 2.0 10^{12} cm^{-3} at the exhaust plane and the atom density in the facility for a back pressure of 2.5 m Pa is 6.0 10^{11} cm^{-3} at 300 K. In this range of back pressure, in the region 10 cm downstream from the exhaust of the SPT, the atom density consists of neutral atoms ejected from the thruster. In the rest of the domain, the atom density is completely controlled by the ambient back pressure of neutrals.

We have compared the electron density in the plume obtained with electrical probes with results from the simulation. Figure 3 gives the variation of the electron density as a function of axial position for two radial positions from the measurements and calculations. Experiment and model give a similar profile of the axial plasma density along the symmetry axis ($r=0$) although the slope of the measured density is larger than in the calculations. The calculated density at $r=60$ mm is almost two times larger than the measured density. This discrepancy could be due to the approximations in the model (constant electron temperature, neglect of the effect of the magnetic field in the exhaust region, and ion distribution at exhaust).

We also compared the model predictions and experimental results obtained with the RPA. The analyzer was positioned at different radial and axial positions in the plume. The zero radial position corresponds to the thruster axis, and the zero axial position is fixed at the exit plane of the SPT. Results of the calculated ion energy distribution functions are compared with experiments in Fig. 4 at an axial position of 421 mm. Note that the energy distribution given by the RPA gives the energy per charge of the ion. Differences between single and double charged ions are not detected by the RPA, and the peak of doubly charged ions is thus mixed with the peak of single-charge ions. Results from both experiment and model give a peak value of the energy distribution for an ion energy of 250 eV. The agreement between measurements and calculations is good in the energy range around the peak; differences appear in the tail of the distribution at low and high energy. One of the reasons for this discrepancy is undoubtedly related to the assumptions on the ion distribution function in the exhaust plane. The population of low-energy ions is significantly larger in the model results. These ions

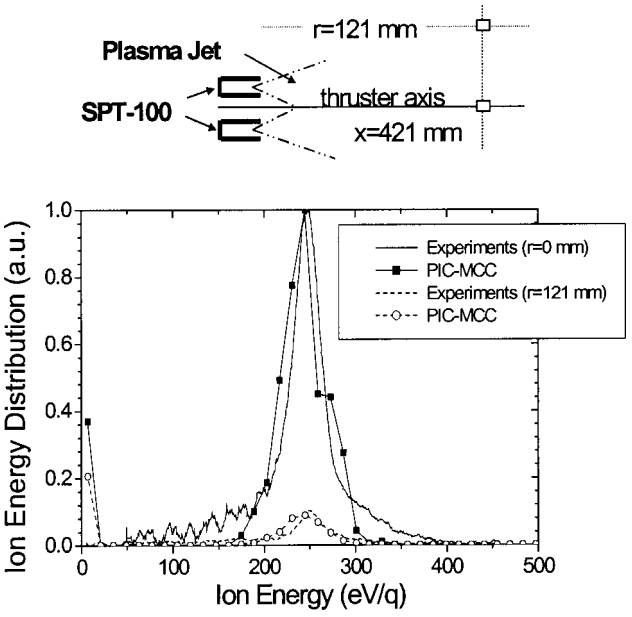

FIG. 4. Ion energy distribution calculated and measured in the PIVOINE facility at two positions in the plume (421 mm from the exhaust plane, on the thruster axis, and at a radial position 121 mm from the axis). Same conditions as Fig. 3.

are created by charge-exchange collisions between fast ions ejected from the thruster and neutral atoms (ejected from the thruster or due to the background pressure in the chamber). The RPA is well adapted to collect ions of directed velocity parallel to the axis of the analyzer. The velocity of ions created by charge-exchange collisions has a non-negligible component normal to the RPA axis. The collection of all of the low-energy ions is therefore difficult with the RPA.

These comparisons show that the model has a good potential for predicting the plume properties. Before performing systematic comparisons, it is however useful to better understand how sensitive the model results are to the assumptions (mainly those related to the ion energy and angular distribution in the exhaust plane). This is the purpose of the next section.

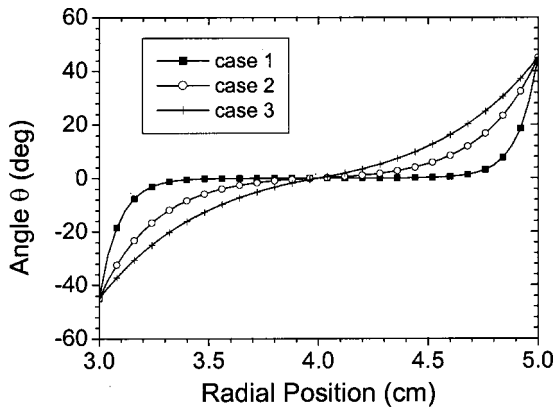

FIG. 5. Three different profiles of the angle of injection used in the simulations.

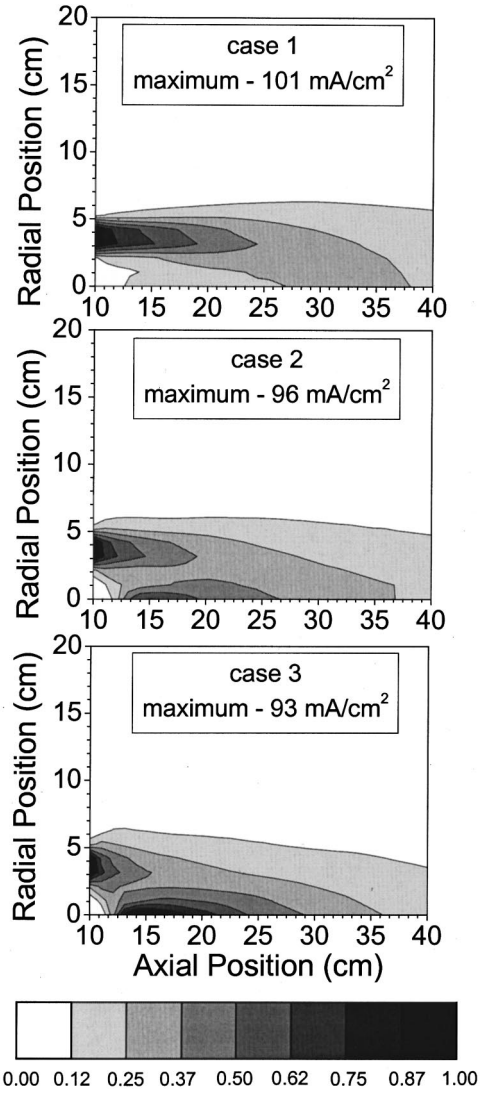

FIG. 6. Contours of constant ion current density J_0 for different angular distributions of the ejected particles (see Fig. 5). The background pressure is 3.3 m Pa. Same conditions as Fig. 3.

V. DISCUSSION ON THE MODEL ASSUMPTIONS AND INPUT PARAMETERS

In this section, we discuss the sensitivity of the results to the assumptions of the model. The ion distribution in the exhaust region is supposed to be a displaced Maxwellian [Eq. (3)] and we study the influence of some of the parameters characterizing this distribution [angular distribution, $\theta(r)$, ion temperature, T_i]. We also discuss the influence of the background pressure and of the electron temperature.

A. Angular distribution of ejected particles

The calculated ion current density is, as expected, strongly affected by the assumed angular distribution of ejected heavy particles $\theta(r)$.

Figure 5 shows three different profiles of $\theta(r)$ for which we performed the plume calculations. These profiles correspond to the distribution of Eq. (6), with a maximum ejection angle θ_m equal to 45°, but with different values for δ. The

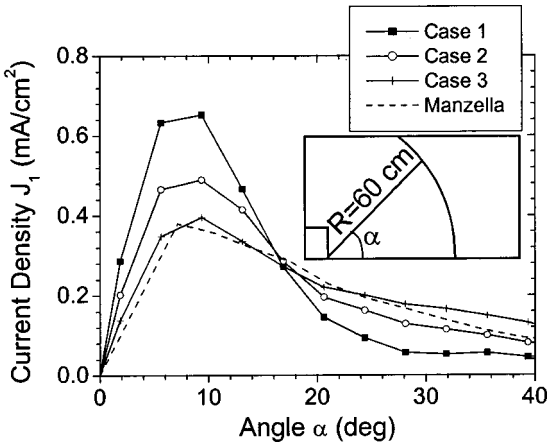

FIG. 7. Influence of the angular distribution on the ion current density for a background pressure of 3.3 m Pa. Calculations are compared with the experimental results of Manzella and Sankovic (see Ref. 19) for a radial position R of 60 cm. Same conditions as Fig. 3.

background pressure is now 3.3 m Pa. All the other parameters are the same as in the previous section.

The calculated spatial distribution of the ion current density for cases 1, 2, and 3 are plotted in Fig. 6. We see that the qualitative aspect of the plume is very different for each case. The peak current density around the axis in a region extending to 15 cm downstream the exhaust plane is much more pronounced in case 3, corresponding to a more divergent beam. Note that similar behavior has been obtained by VanGilder, Boyd, and Keidar, changing the maximum divergence angle of injection of particles.[8]

From these calculations we can deduce the current density distribution $J_0(R,\alpha)$ on a sphere of radius R and centered on the symmetry axis in the exhaust plane, and as a function of the angle α defined in Fig. 7. Most experimentalists use this representation of the current-density distribution. Here, we use a slightly different representation where we plot the same current density multiplied by $\sin\alpha$, i.e., $J_1(R,\alpha)=\sin\alpha J_0(R,\alpha)$. J_1 is proportional to the current dI_1 collected along a ring between (R,α) and $(R,\alpha+d\alpha)$ on the sphere of radius R and defined by: $dI_1 = 2\pi R^2 J_0(R,\alpha)\sin\alpha d\alpha$. In this representation the divergent (large α) ions are more visible.

The calculated current-density distribution J_1 at $R=60$ cm is represented in Fig. 7 for cases 1, 2, and 3 (for α less than 40°). The current density measured by Manzella and Sankovic,[19] is represented on the same figure for comparison. The ion current density was measured by Manzella and Sankovic using a rotating probe for different SPT prototypes and for various background pressure in nominal conditions (applied voltage of 300 V and a discharge current of 4.5 A). The experimental measurements reproduced in Fig. 7 correspond to a SPT-100 manufactured by Fakel and a background pressure of 3.3 mPa. We see in Fig. 7 that the best agreement between the simulations and the measurements of Manzella and Sankovic for α less than 40° obtained for case 3.

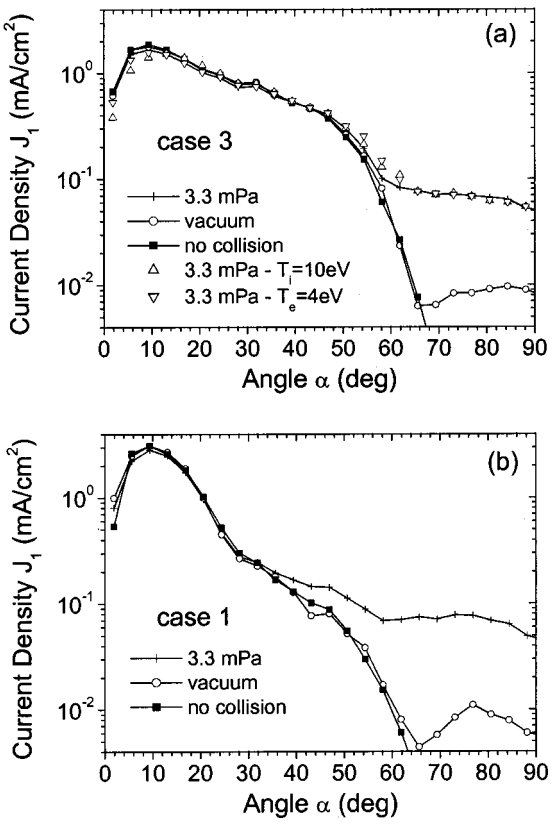

FIG. 8. (a) Ion current-density distribution J_1 $(=J_0\sin\alpha)$ as a function angle α, for the angular distribution of case 3 (Fig. 6). The radial position R is 30 cm. Same conditions as Fig. 3. (b) Ion current-density distribution J_1 $(=J_0\sin\alpha)$ as a function angle α, for the angular distribution of case 1 (Fig. 6). The radial position R is 30 cm. Same conditions as Fig. 3.

B. Effect of background pressure and other parameters

It is interesting to study the influence of the background pressure on the ion current-density distribution J_1. Figures 8(a) and 8(b) show the ion current density J_1 at $R=30$ cm, as a function of α, for α between 0° and 90°, and for cases 3 and 1, respectively. The current density is plotted for a background pressure of 3.3 m Pa, for a zero background pressure (''vacuum''), and assuming no ion-neutral collisions (i.e., with zero background pressure *and* neglecting collisions with neutral atoms ejected from the thruster). It is very instructive to see that up to $\alpha=50°$, there is practically no difference between the three cases (3.3 m Pa, zero background pressure, and no collisions). Similar conclusions using the PIC-DSMC model have been obtained and reported by Boyd[9] (the background pressure was 2 m Pa in Ref. 9). This is because for these relatively low angles the ion beam is mainly composed of energetic ions coming from the exhaust plane. For small enough angles, the ion beam is practically not perturbed by the collisions or by the potential distribution in the plume (the beam energy is large with respect to the potential variations inside the plume). The measured current for α less than 40° or 50° [this limit depends on $\theta(r)$] is therefore directly related to the ion current distribution in the exhaust plane. For larger values of the angle α, the measured current distribution becomes much more sensitive to collisions. It is clear

from Fig. 8 that, with the assumed form of the angular distribution $\theta(r)$ in the exhaust plane, the ion current measured at angles larger than 50° only corresponds to low-energy ions created by charge-exchange collisions in the plume (when no ion-neutral collisions are taken into account, the ion current for α larger than 60° quickly goes to zero). For a background pressure of 3.3 m Pa, typical of the PIVOINE facility, the ion current at large angles is entirely controlled by charge-exchange collisions between the ejected ions and the neutral atoms from the residual background pressure [the ion current density for α larger than 60° is one order of magnitude larger in the 3.3 m Pa case than in the 0 m Pa (''vacuum'') case].

It also appears in Fig. 8(a) that the ion current density is essentially not sensitive to the electron and ion temperatures in the ranges 2–4 and 4–10 eV, respectively. This is because the generation of low-energy ions through charge-exchange collisions is not very sensitive to these parameters. However, the calculations show, as in Ref. 8, that the ion energy flux is sensitive to the electron temperature (since the potential drop in the plume is directly proportional to the electron temperature, the energy gained by the charge-exchange ions is simply related to the electron temperature).

C. Backscattered ions

One of the issues of plume simulations is the estimation of the flux and energy flux of the ions that may be backscattered toward the satellite and cause damage to sensitive parts such as the solar panels. We have therefore calculated the backscattered ion current density through the plane perpendicular to the thruster axis and containing the channel exhaust [exhaust plane, see Fig. 9(a)].

Figure 9(a) shows the calculated backscattered ion current density for case 1 and case 3 with a background pressure of 3.3 m Pa while Fig. 9(b) shows the same currents in the case of vacuum (zero background pressure). We see [Fig. 9(a)] that the backscattered ion current densities for case 1 and case 3 are very similar for a background pressure of 3.3 m Pa. This is consistent with the results above for $J_1(R,\alpha)$. The backscattered ion flux in that case is the result of charge-exchange collisions between beam ions and background atoms due to the residual pressure in the chamber. These collisions somewhat erase the ''memory'' of the angular distribution of ions ejected from the channel. In real conditions in space, the residual pressure is almost zero and the calculated backscattered ion current density is much more sensitive to the details of the initial angular distribution of the ions and atoms ejected from the thruster, as can be seen in Fig. 9(b). The backscattered ion current density is much larger for the more divergent ion beam (case 1) than for the other case (case 3). Note also the much larger value of the backscattered ion current density for 3.3 m Pa [compare the units in Figs. 9(a) and 9(b)].

Other calculations with *and* without backpressure (not shown here) also indicate that the backscattered ion current densities are not sensitive to the ion-beam temperature, T_i, and electron temperature in the plume, T_e, in the ranges 4–10 and 2–4 eV, respectively.

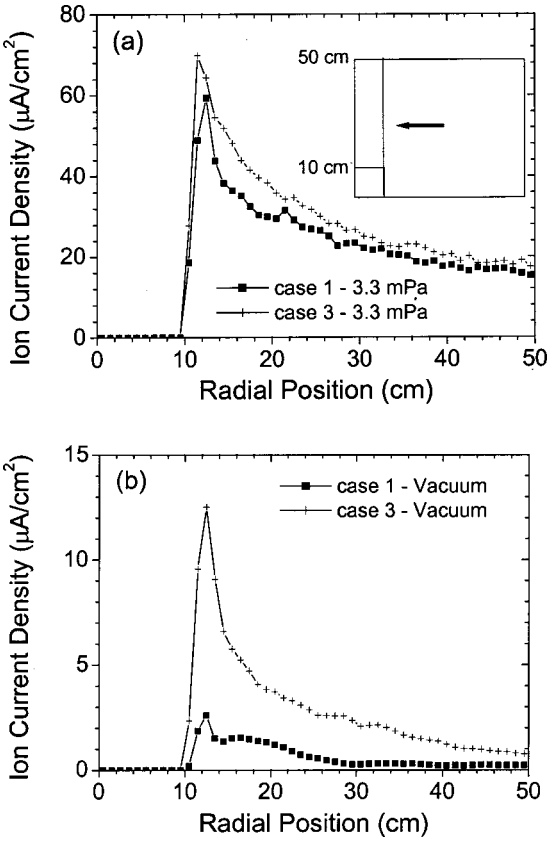

FIG. 9. (a) Current density of backscattered ions as a function of radial position along the exhaust plane for 3.3 m Pa background pressure and for two angular distributions. Same conditions as Fig. 3. (b) Current density of backscattered ions as a function of radial position along the exhaust plane for a zero background pressure and for two angular distributions. Same conditions as Fig. 3.

VI. CONCLUSION

The conclusions of the present article can be summarized as follows:

(1) The results of the PIC-MCC model (which neglects the influence of collisions on the neutral atom velocity distribution in the plume) for the SPT plume are in good agreement with the predictions of the more accurate but more time-consuming DSMC model.

(2) The results of the simulations are very sensitive to the assumed distribution of ions (and neutral atoms) ejected from the thruster. The angular distribution of these ions is especially important. The beam current density for small divergence angles is simply related to the current density of the ions ejected from the thruster. It should therefore be possible to deduce the current density in the exhaust plane, of ions ejected with angles less than 40° from measurements of the angular distribution of the ion current density in the plume.

(3) It is very difficult to extract useful information on the ion current distribution at large divergence angles from experiments performed in an on-ground facility where the background pressure is on the order of a few m Pa. In this pressure range, the ion current distribution at large angles, and the backscattered ion current density are completely controlled by charge-exchange collisions between beam ions and neutral background atoms. Under vacuum conditions, the

backscattered ion current density is strongly dependent on the distributions of ions and atoms ejected from the channel. Measurements under flight conditions using probes at large divergence angles on STENTOR[7] will be useful to provide necessary data to compare calculations and experimental results. These measurements will help to validate the initial distribution of the heavy particles in flight conditions.

(4) Parameters such as the electron temperature in the plume and the temperature of the ejected ions moderately influence the ion current-density distribution in the plume (when they are varied within a reasonable range). However, the distribution of electric potential and plasma density in the plume, as well as the ion energy flux distributions are obviously dependent on the electron temperature.

The simulations performed in this article neglect the potential drop between the channel exhaust and the cathode outside the channel. Also, a possible increase of electric potential between the cathode region and the plume was not considered. If the magnetic field is not small in the cathode region, such a potential increase may be necessary to extract the electrons that are needed for neutralizing the ion beam in the plume.[20] Finally, ionization outside the channel is possible and may be a non-negligible (compared with charge-exchange collisions) source of low-energy ions the plume near field. All these issues do not alter the conclusion above. However, proper answers to these questions are needed. These issues must be addressed with the help of 2D models of the thruster including the channel and the near-field plume.[21,22]

ACKNOWLEDGMENTS

This work is supported by CNES under Contract No. 712/98/CNES/7487/00. The authors thank the Laboratoire d'Aérothermique, CNRS-UPR9020 in Orléans, for providing the experimental data.

[1] F. Darnon, L. Petitjean, J. P. Diris, J. Hoarau, L. Torres, and T. Grassin, 27th International Electric Propulsion Conference, Pasadena, CA, 2001, paper IEPC-01-167.
[2] J. Duning and J. Sankovic, 36th AIAA Joint Propulsion Conference, Huntsville, AL, 2000, paper AIAA-00-3145.
[3] G. Saccoccia, 36th AIAA Joint Propulsion Conference, Huntsville, AL, 2000, paper AIAA-00-3149.
[4] A. Cadiou, C. Gélas, F. Darnon, L. Jolivet, and N. Pillet, 27th International Electric Propulsion Conference, Pasadena, CA, 2001, paper IEPC-01-008.
[5] A. Bouchoule, C. Philippe-Kadlec, M. Prioul, F. Darnon, M. Lyszyk, L. Magne, D. Pagnon, S. Roche, M. Touzeau, S. Béchu, P. Lasgorceix, N. Sadéghi, N. Dorval, J. P. Marque, and J. Bonnet, Plasma Sources Sci. Technol. **10**, 364 (2001).
[6] J. P. Boeuf and L. Garrigues, J. Appl. Phys. **84**, 3541 (1998); L. Garrigues, A. Héron, J. C. Adam, and J. P. Boeuf, Plama Sources Sci. Technol. **9**, 219 (2000).
[7] F. Darnon, 36th AIAA Joint Propulsion Conference, Huntsville, AL, 2000, paper AIAA-00-3525.
[8] D. B. VanGilder, I. D. Boyd, and M. Keidar, J. Spacecr. Rockets **37**, 129 (2000).
[9] I. D. Boyd, J. Spacecr. Rockets **38**, 381 (2001).
[10] D. B. VanGilder and I. D. Boyd, 26th International Electric Propulsion Conference, Kitakyushu, Japan, 1999, paper IEPC-99-076.
[11] G. A. Bird, *Molecular Gas Dynamics and the Direct Simulation of Gas Flows*, (Oxford University, New York, 1994).
[12] D. Y. Oh, D. E. Hastings, C. M. Marrese, J. M. Haas, and A. D. Gallimore, J. Propul. Power **15**, 345 (1999).
[13] S. Qarnain and M. Martinez-Sanchez, 34th AIAA Joint Propulsion Conference, Cleveland, OH, 1998, paper AIAA-98-3796.
[14] V. M. Gavryushin and V. Kim, Soviet Phys. Tech. **26**, 505 (1981) [Zh. Teck. Fiz. **51**, 850 (1981).
[15] I. D. Boyd, J. Propul. Power **16**, 902 (2000).
[16] M. Touzeau, M. Prioul, S. Roche, N. Gascon, C. Pérot, F. Darnon, S. Béchu, C. Philippe-Kadlec, L. Magne, P. Lasgorceix, D. Pagnon, A. Bouchoule, and M. Dudeck, Plasma Phys. Controlled Fusion **42**, B323 (2000).
[17] L. Garrigues, I. D. Boyd, and J. P. Boeuf, J. Propul. Power **17**, 772 (2001).
[18] C. Pérot, N. Gascon, S. Béchu, P. Lasgorceix, M. Dudeck, L. Garrigues, and J. P. Boeuf, 35th AIAA Joint Propulsion Conference, Los Angeles, CA, 1999, paper AIAA-99-2716.
[19] D. H. Manzella and J. M. Sankovic, 31st AIAA Joint Propulsion Conference, San Diego, CA, 1995, paper AIAA-95-2927.
[20] M. Keidar and I. D. Boyd, J. Appl. Phys. **86**, 4786 (1999).
[21] J. M. Fife, Ph.D. Thesis, Massachusetts Institute of Technology, MA, 1998.
[22] G. J. M. Hagelaar, J. Bareilles, L. Garrigues, and J. P. Boeuf, J. Appl. Phys. **91**, 5592 (2002).